Influence of molecular topology on the static and dynamic properties of single polymer chain in solution

Cuiliu Fu, Wenze Ouyang, Zhaoyan Sun, and Lijia An

Citation: J. Chem. Phys. **127**, 044903 (2007); doi: 10.1063/1.2750338
View online: http://dx.doi.org/10.1063/1.2750338
View Table of Contents: http://jcp.aip.org/resource/1/JCPSA6/v127/i4
Published by the American Institute of Physics.

Influence of molecular topology on the static and dynamic properties of single polymer chain in solution

Cuiliu Fu
State Key Laboratory of Polymer Physics and Chemistry, Changchun Institute of Applied Chemistry, Chinese Academy of Sciences, Changchun 130022, People's Republic of China

Wenze Ouyang
Fachbereich C Mathematik und Naturwissenschaften, Bergische Universität, D-42097 Wuppertal, Germany

Zhaoyan Sun[a),b)] and Lijia An[a),c)]
State Key Laboratory of Polymer Physics and Chemistry, Changchun Institute of Applied Chemistry, Chinese Academy of Sciences, Changchun 130022, People's Republic of China

(Received 7 February 2007; accepted 25 May 2007; published online 25 July 2007)

The influence of molecular topology on the structural and dynamic properties of polymer chain in solution with ring structure, three-arm branched structure, and linear structure are studied by molecular dynamics simulation. At the same degree of polymerization (N), the ring-shaped chain possesses the smallest size and largest diffusion coefficient. With increasing N, the difference of the radii of gyration between the three types of polymer chains increases, whereas the difference of the diffusion coefficients among them decreases. However, the influence of the molecular topology on the static and the dynamic scaling exponents is small. The static scaling exponents decrease slightly, and the dynamic scaling exponents increase slightly, when the topology of the polymer chain is changed from linear to ring-shaped or three-arm branched architecture. The dynamics of these three types of polymer chain in solution is Zimm-like according to the dynamic scaling exponents and the dynamic structure factors. © *2007 American Institute of Physics*. [DOI: 10.1063/1.2750338]

I. INTRODUCTION

Polymers are ubiquitous in daily life, and a lot of living products are made of synthesized or natural polymers. The polymer architecture strongly affects its physical properties, and then influences the material performance greatly.

For polymer melts, the influence of chain topology on the static and dynamic properties had been abundantly investigated. Ring-shaped chains are more compact, interpenetrateless, and diffuse faster than the linear counterparts. The ring-shaped chains have the static scaling relationships $R_g \sim N^{0.42}$ for the radius of gyration and $R_e \sim N^{0.41}$ for the mean diameter.[1,2] However, for linear and branched chains, the scaling relationship of the radius of gyration is $R_g \sim N^{0.5}$. Moreover, the scaling relationship of diffusion coefficient has two different regimes for the linear and the ring-shaped chains.[1,2] The center of mass diffusion coefficient $D_{\mathrm{c.m.}}$ of linear chains shorter than a crossover chain length N_c scales as $D_{\mathrm{c.m.}} \sim N^{-1}$, while that of linear chains longer than N_c scales as $D_{\mathrm{c.m.}} \sim N^{-2}$. Brown and Szamel[1,2] indicated that short ring-shaped chains also have $D_{\mathrm{c.m.}} \sim N^{-1}$, but for longer ring-shaped chains $D_{\mathrm{c.m.}}$ scales as $D_{\mathrm{c.m.}} \sim N^{-1.54}$. Hur *et al.*[3] showed that the ring-shaped chains diffuse slower for short chains but faster for long chains than the linear chains. Therefore, the static and dynamic properties of polymer chains in melt change obviously as a result of the molecular topology difference.

The single ring-shaped chain in solution was studied by Monte Carlo simulation with bond fluctuation algorithm which gives $R_g \sim N^{0.595}$ and $R_e \sim N^{0.605}$ by Müller *et al.*[4] and $R_g \sim N^{0.58}$ and $R_e \sim N^{0.585}$ by Brown *et al.*,[5] by an off-lattice model[6] which gives $R_e \sim N^{0.555}$ and by Bensafi *et al.*[7] which gives $R_g \sim N^{0.6}$. These results indicate that the static properties of a single ring-shaped chain in solution are very similar to those of a linear chain. The three-arm branched chain in solution was also studied, showing $R_g \sim N^{0.6}$ by Brown and Szamel[8] and $R_g \sim N^{0.587}$ by Sikorski.[9] However, the above simulations neglected the hydrodynamic interaction (HI) and predicted Rouse-like behavior of chain diffusion. Grest *et al.*[10] also found the Rouse-like diffusion of the branched polymer chain without considering the hydrodynamic interaction. Taking into account HI, Dünweg and Kremer[11,12] found Zimm scaling for a linear polymer chain in solution using molecular dynamics (MD) simulations.

Stimulated by the previous studies, in this paper, we investigate the static and the dynamic properties of single ring-shaped, three-arm branched, and linear polymer chains in solution using MD simulations. The results may be helpful to understand the presence or not of other type of chains in polymer solution.[13] Model and simulation details are given in Sec. II, and the results and discussion are presented in Sec. III. Finally, we summarize our results in Sec. IV.

[a)]Authors to whom correspondence should be addressed.
[b)]Tel.: +86-431-85262896; Fax: +86-431-85262969. Electronic mail: zysun@ciac.jl.cn
[c)]Tel.: +86-431-85262206; Fax: +86-431-85685653. Electronic mail: ljan@ciac.jl.cn

TABLE I. The static and dynamic properties of ring-shaped, three-arm branched, and linear polymer chains in solution. N, R_g, R_h, and $D_{\mathrm{c.m.}}$ are the degree of polymerization, the radius of gyration, the hydrodynamic radius, and the center of mass diffusion coefficient of the polymer chain, respectively. τ is the relaxation time for the chain diffusing its own size. R_f is the end-to-end distance for the linear polymer chain. R_e is the mean radius of the ring polymer chain. L is the length of one side of the cubic box.

		Ring-shaped chain					Three-arm branched chain				Linear chain				
N	L	R_e	R_g	R_h	$D_{\mathrm{c.m.}}\times 10^3$	$\tau/10$	R_g	R_h	$D_{\mathrm{c.m.}}\times 10^3$	$\tau/10$	R_f	R_g	R_h	$D_{\mathrm{c.m.}}\times 10^3$	$\tau/10$
6	16.8	1.71	0.91	1.52	26.6	0.52	1.10	1.69	22.0	0.92	2.80	1.17	1.74	23.5	0.97
8	16.8	2.02	1.08	1.60	21.4	0.91	1.26	1.75	18.7	1.43	3.38	1.39	1.83	18.9	1.72
10	16.8	2.30	1.23	1.69	18.7	1.36	1.43	1.84	17.1	1.99	3.96	1.61	1.94	16.0	2.69
12	16.8	⋯	⋯	⋯	⋯	⋯	⋯	⋯	⋯	⋯	4.48	1.81	2.05	14.9	3.67
16	16.8	3.01	1.62	1.97	12.8	3.43	1.91	2.15	12.0	5.07	5.35	2.15	2.26	11.6	6.7
20	16.8	3.48	1.88	2.16	10.5	5.61	2.18	2.34	10.4	7.59	6.19	2.50	2.47	9.29	11.2
24	16.8	3.80	2.07	2.30	9.6	7.67	2.47	2.53	8.61	11.9	6.78	2.73	2.62	9.21	13.5
28	16.8	4.22	2.29	2.47	8.44	10.4	2.67	2.67	7.39	16.1	7.61	3.06	2.83	7.19	21.7
30	16.8	4.41	2.39	2.55	7.54	12.7	2.81	2.77	7.15	18.4	8.23	3.20	2.95	6.95	24.7
36	16.8	4.92	2.67	2.77	7.53	15.9	3.13	2.99	6.36	25.7	8.62	3.51	3.15	6.11	33.8
40	16.8	5.16	2.82	2.89	5.98	22.2	3.29	3.13	5.45	33.3	9.57	3.82	3.32	5.63	43.4
50	22.0	5.95	3.24	3.22	5.78	30.4	3.92	3.49	5.29	46.1	11.3	4.43	3.70	5.50	59.6
60	22.0	6.48	3.57	3.49	4.9	43.4	4.41	3.88	4.56	71.3	12.3	4.95	4.03	4.37	93.8
70	22.0	7.15	3.94	3.77	4.56	56.8	4.68	4.11	3.93	93	13.5	5.27	4.29	3.93	118
80	22.0	7.98	4.65	4.09	3.95	80.2	5.12	4.40	3.53	123	15.4	5.91	4.61	3.32	175
90	22.0	8.43	4.62	4.31	3.55	100	5.29	4.58	2.95	158	15.6	6.19	4.92	2.97	215
100	22.0	8.99	4.91	4.55	2.93	137	5.59	4.78	2.82	185	15.3	6.37	5.09	2.63	257

II. MODEL AND SIMULATION DETAILS

In the simulations, the degree of polymerization (N) of each type of polymer chain changes from 6 to 100. All the particles (including monomer and solvent particles) interact with each other via the Lennard-Jones potential,[14]

$$U_{\mathrm{LJ}}(r)=\begin{cases}4\varepsilon\left[\left(\dfrac{\sigma}{r}\right)^{12}-\left(\dfrac{\sigma}{r}\right)^{6}\right], & r<r_c\\ 0, & r\geqslant r_c.\end{cases} \tag{1}$$

The parameter ε governs the strength of the interaction and σ defines a length scale. For convenience, the reduced units are used in this paper, where σ, ε, and m (the mass of a solvent particle) are set to be unity. Time is measured in unit of $\tau_{\mathrm{LJ}}=(m\sigma^2/\varepsilon)^{1/2}$. The mass of a monomer particle is chosen to be twice of a solvent particle. The cutoff diameter is $r_c=2^{1/6}\sigma$ for computation efficiency.

The polymer chains are described by the bead-spring model, in which neighboring monomers interact with each other via finitely extensible nonlinear elastic potential,

$$U_{\mathrm{ch}}(r)=-\frac{k}{2}R_0^2\ln\left(1-\frac{r^2}{R_0^2}\right). \tag{2}$$

Here r is the distance between the nearest monomers along the chain backbone, k is the spring constant which takes the value of 7.0 in reduced unit, and R_0 is the ultimate bond length with $R_0=2.0$.[11]

The equations of motion are integrated using the leap-frog algorithm[14] with the integration time step $\delta_t=0.006\tau_{\mathrm{LJ}}$. The particle number density is selected to be $\rho=0.8638$ according to Ref. 11 and the temperature is $k_BT=1.2$, which is controlled via Berendsen thermostat and the relaxation time $\tau_T=1.2\tau_{\mathrm{LJ}}$.[15] The force imposed on a particle is

$$f=\begin{cases}-\left(\dfrac{\partial U_{\mathrm{LJ}}}{\partial r}\right) & \text{for } r<r_c\\ 0 & \text{for } r\geqslant r_c,\end{cases} \tag{3a}$$

for solvent, and

$$f=\begin{cases}-\left(\dfrac{\partial U_{\mathrm{LJ}}}{\partial r}+\dfrac{\partial U_{\mathrm{ch}}}{\partial r}\right) & \text{for } r<r_c\\ -\dfrac{\partial U_{\mathrm{ch}}}{\partial r} & \text{for } r\geqslant r_c,\end{cases} \tag{3b}$$

for monomer.

The diffusion coefficient of the polymer chain is remarkably influenced by the size of the simulation box,[11,16] which is given by

$$D_{\mathrm{c.m.}}=\frac{k_BT}{\eta_sR_g}\left[\frac{8}{3(6\pi^3)^{1/2}}-\frac{2}{9\pi}\frac{R_g}{L}\right], \tag{4}$$

where η_s is the viscosity of pure solvent. To diminish the difference of the finite size effects for different polymer chain lengths, according to Eq. (4), we need to enlarge the simulation box from $L=16.8$ (L is the length of the box side) for chains with $N<50$ to $L=22.05$ for chains with $100\geqslant N\geqslant 50$. Consequently, the number of particle changes from 4096 to 9261 when enlarging the simulation box. For the sake of computation efficiency, the cell index method[14] is employed to accelerate the calculation. After relaxing 1.5×10^6 time steps, the system reaches equilibrium and the physical properties are recorded every 200 time steps in 6.0×10^6 time step production run (1 time step$=0.006\tau_{\mathrm{LJ}}$).

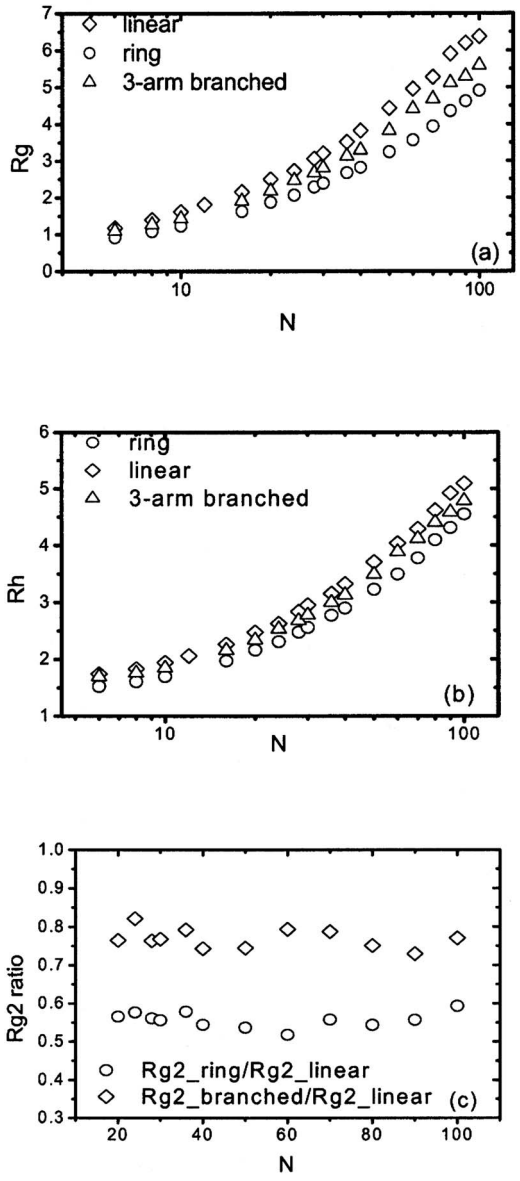

FIG. 1. Plot for (a) the radius of gyration R_g, (b) the hydrodynamic radius R_h for the ring-shaped chain (circle), the three-arm branched chain (triangle), and linear polymer chain (diamond), and (c) the ratios of R_g^2 of ring or three-arm branched polymer to that of linear counterpart vs the degree of polymerization N.

III. RESULTS AND DISCUSSION

To manifest the influence of the molecular topology on the static and dynamic properties of single polymer chain in solution, we calculate the end-to-end distance for the linear chain, the mean square diameter for the ring-shaped chain, and the radius of gyration, the hydrodynamic radius, the diffusion coefficient, the relaxation time, and the static and the dynamic structure factors for the three types of polymer chains. The mean square end-to-end distance[17] is defined by

$$\langle R_f^2 \rangle = \langle (\mathbf{r}_N - \mathbf{r}_1)^2 \rangle, \tag{5}$$

where $\mathbf{r}_1$ and $\mathbf{r}_N$ are the position vectors of the first and the last monomers, respectively. The mean square diameter[2] for the ring-shaped polymer is given by

TABLE II. The conformation of the ring-shaped, the three-arm branched, and the linear polymer chains in solution. Here a, b, and c represent the largest, the middle, and the smallest components of R_g along the X, Y, and Z axes, respectively.

	N	b/a	c/a	c/b
Linear	10	0.747 877	0.551 108	0.748 686
	30	0.730 876	0.529 009	0.740 567
	60	0.743 552	0.545 711	0.746 84
Branched	10	0.800 162	0.611 94	0.773 136
	30	0.786 797	0.604 963	0.778 717
	60	0.780 622	0.592 047	0.769 623
Ring shaped	10	0.816 566	0.642 907	0.793 814
	30	0.806 331	0.635 311	0.794 147
	60	0.811 351	0.639 046	0.795 921

$$\langle R_e^2 \rangle = \langle (\mathbf{r}_n - \mathbf{r}_{n+N/2})^2 \rangle, \tag{6}$$

where $\mathbf{r}_n$ is the position vector of the nth monomer. The mean square radius of gyration[17] and the hydrodynamic radius[11] for the three types of polymer chains are

$$\langle R_g^2 \rangle = \frac{1}{2N^2} \sum_{m=1} \sum_{n=1} (\mathbf{r}_n - \mathbf{r}_m)^2 \tag{7}$$

and

$$\left\langle \frac{1}{R_h} \right\rangle = \frac{1}{N^2} \sum_{m \neq n} \left\langle \frac{1}{r_{mn}} \right\rangle, \tag{8}$$

respectively, where r_{mn} is the distance between the mth and the nth monomers.

The center of mass diffusion coefficient and the relaxation time[18] of the polymer chain in solution are calculated via

$$6D_{\text{c.m.}}t = \langle (\mathbf{r}_{\text{c.m.}}(t) - \mathbf{r}_{\text{c.m.}}(0))^2 \rangle, \tag{9}$$

$$\tau = R_g^2/(6D_{\text{c.m.}}), \tag{10}$$

where $D_{\text{c.m.}}$ is the diffusion coefficient of the mass center of the polymer chain, $\mathbf{r}_{\text{c.m.}}(t)$ is the position vector of the mass center of the polymer chain at time t, and τ is the relaxation time for the polymer chain diffusing its own size.

The static structure factor $S(k)$ and the dynamic structure factor $S(k,t)$ of the polymer chain in solution[11] can be calculated via

$$S(k) = N^{-1} \sum_{ij} \langle \exp(i\mathbf{k} \cdot \mathbf{r}_{ij}) \rangle = N^{-1} \sum_{ij} \frac{\sin(kr_{ij})}{kr_{ij}} \tag{11}$$

and

$$S(k,t) = N^{-1} \sum_{ij} \langle \exp\{i\mathbf{k} \cdot [\mathbf{r}_i(t) - \mathbf{r}_j(0)]\} \rangle$$

$$= N^{-1} \sum_{ij} \frac{\sin(k|r_i(t) - r_j(0)|)}{k|r_i(t) - r_j(0)|}, \tag{12}$$

where $r_{ij} = |\mathbf{r}_i - \mathbf{r}_j|$ is the distance between the ith and the jth monomers.

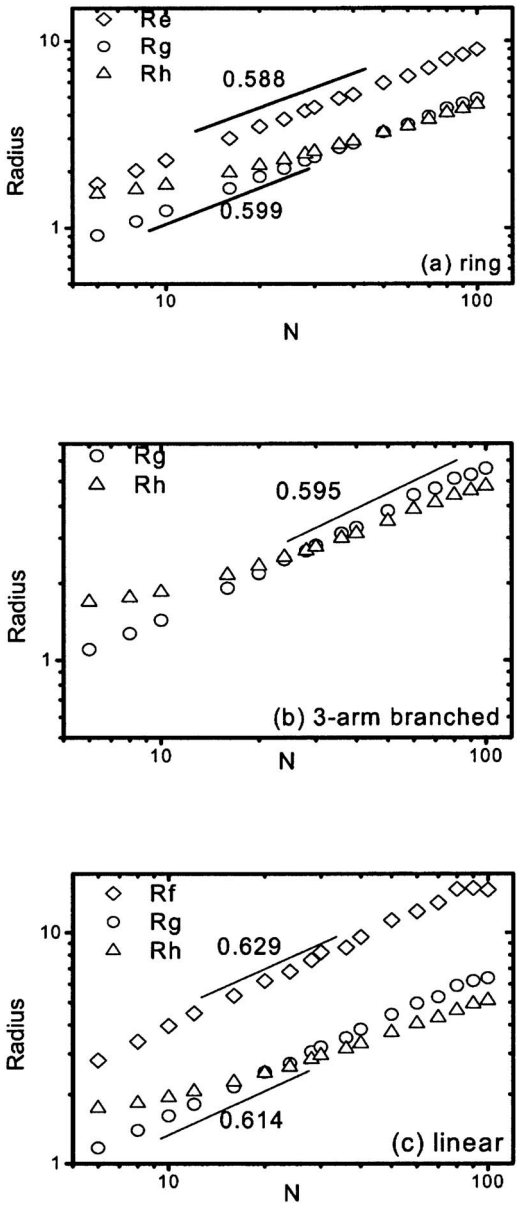

FIG. 2. The static scaling relationships for the polymer chain in solution. The radii of the polymer chain are plotted as functions of N for (a) the ring-shaped chain, (b) the three-arm branched chain, and (c) the linear chain.

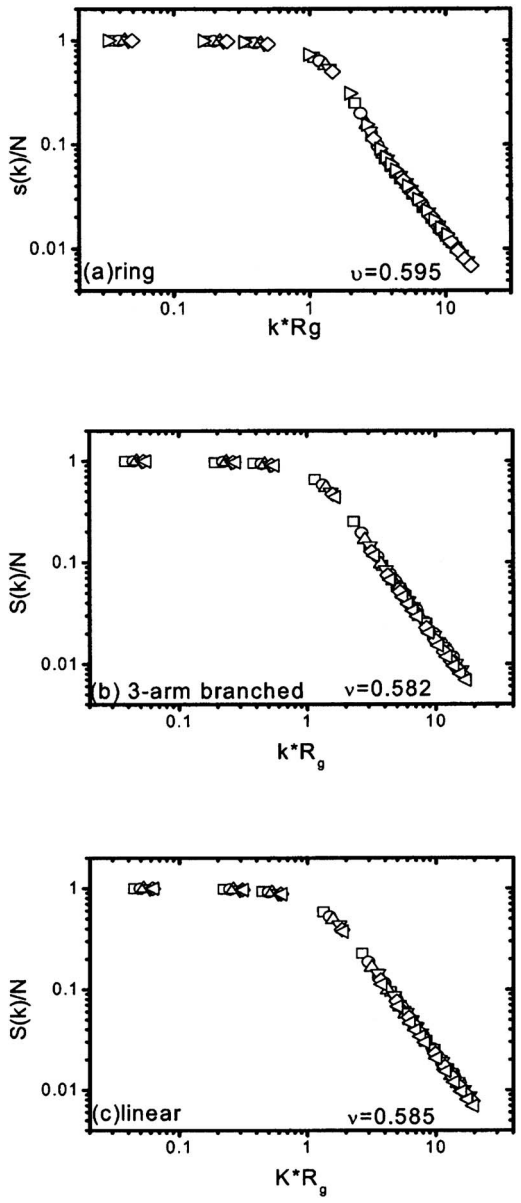

FIG. 3. The static structure factor $S(k)/N$ as a function of wave number weighted radius of gyration kRg. (a) is for ring-shaped chain, (b) for three-arm branched chain, and (c) for linear chain. Different symbols represent polymer chains with different N.

A. The static properties

The static properties of the ring-shaped, the three-arm branched, and the linear polymer chains are listed in Table I. The results for the linear chain are in agreement with those from Ref. 11, in which the single linear polymer chain with $N=30$, 40, and 60 in solution was studied by MD. Figure 1 shows the dependence of R_g and R_h of the three types of polymer chains on N. It is shown that the differences of the sizes among the three types of polymer chains increase with increasing N. At the same degree of polymerization, the ring-shaped chain is the most compact, and the linear chain is the most stretched. Furthermore, the ratios for the R_g^2 of ring-shaped or three-arm branched chain to that of linear chain as a function of degree of polymerization are obtained [Fig. 1(c)]. It is shown that the ratios are similar in the range of $N=20$ to $N=100$ for ring and three-arm branched polymers. Therefore, the mean ratios $\langle\langle R_g^2\rangle_r/\langle R_g^2\rangle_l\rangle=0.558$ for the ring-shaped chain and $\langle\langle R_g^2\rangle_b/\langle R_g^2\rangle_l\rangle=0.769$ for the three-arm branched chain can be obtained for $20\leqslant N\leqslant 100$. These results are in agreement with the result from Ref. 19. Zimm and Stockmayer[13] also predicted the ratios $\langle R_g^2\rangle_r/\langle R_g^2\rangle_l=0.5$ and $\langle R_g^2\rangle_b/\langle R_g^2\rangle_l=0.782$ for ideal ring-shaped and three-arm branched polymer chains, respectively. It indicates that in this simulation, the ring-shaped chains are far from ideal compared with the branched ones.

Table II shows the information about the conformation of the chains. Here, a, b, and c represent the mean value of the largest, the middle, and the smallest components of R_g along the X, Y, and Z axes of every configuration, respectively.[20] It is shown in Table II that the ring-shaped, the three-arm branched, and the linear polymer chains in solution all behave as ellipsoids. The ring-shaped chain pos-

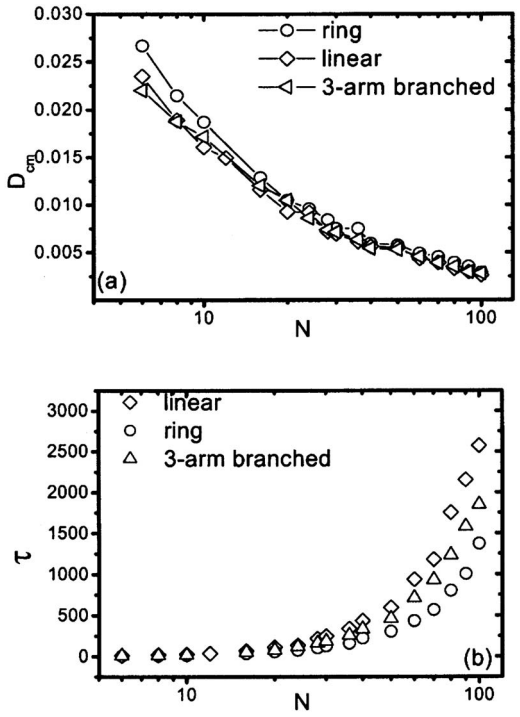

FIG. 4. (a) The diffusion coefficient and (b) the relaxation time of the ring-shaped chain (circle), the three-arm branched chain (triangle), and the linear chain (diamond).

sesses the largest ratios $\langle b/a \rangle$ or $\langle c/a \rangle$, and the linear chain possesses the smallest anisotropic ratios for polymer chains with $N=10,30,60$. The linear chain has free ends but no branched unit; thus it is easier to be stretched in solution than the ring-shaped and the three-arm branched chains. Then the ring-shaped and the three-arm branched chains are more isotropic on conformation and behave as thicker ellipsoids.

For polymer chain in dilute solution, the R_g should obey $R_g \sim (N-1)^{\nu}$ with $\nu=3/5$ in three dimensions.[17] Figure 2

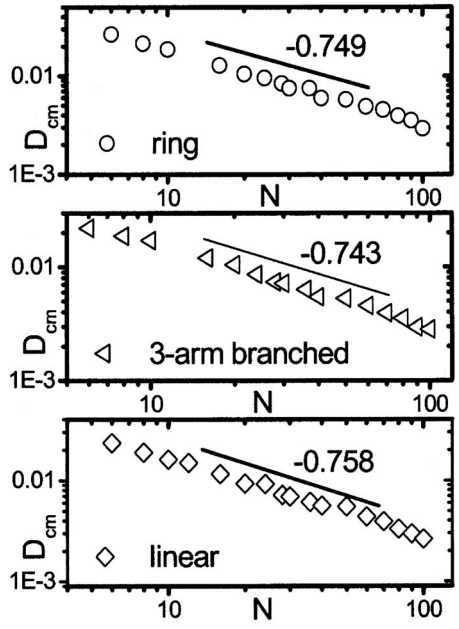

FIG. 5. Diffusion coefficients for the ring-shaped chain (up), the three-arm branched chain (middle), and the linear polymer chain (bottom).

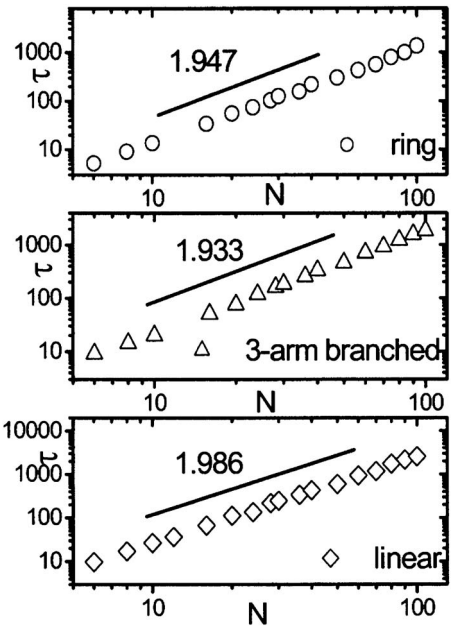

FIG. 6. Relaxation times for the ring-shaped chain (up), the three-arm branched chain (middle), and the linear polymer chain (bottom).

shows the scaling relationships of R_g, R_e, and R_h for the ring-shaped chain, R_g and R_h for the three-arm branched chain, and R_g, R_f, and R_h for the linear polymer chain in solution. We find that $R_g \sim N^{0.599}$ and $R_e \sim N^{0.588}$ for the ring-shaped chain [Fig. 2(a)], $R_g \sim N^{0.595}$ for the three-arm branched chain [Fig. 2(b)], and $R_g \sim N^{0.614}$ and $R_f \sim N^{0.629}$ for the linear chain [Fig. 2(c)]. These scaling exponents are all in accordance with the Flory exponent 3/5. Moreover, the scaling exponents of R_g decrease from 0.614 for the linear chain to 0.599 for the ring-shaped chain and to 0.595 for the three-arm branched chain. It may be attributed to the existence of additional constrains, i.e., there is no free ends in the ring-shaped chain, and there is a grafting point in the three-arm branched chain.

The scaling of R_h is remarkably influenced by the polymer chain length following[21]

$$\left\langle \frac{1}{R_h} \right\rangle = \frac{A}{N^{\nu}} \left(1 - \frac{B}{N^{1-\nu}} + \cdots \right). \tag{13}$$

As long as the polymer chain is long enough, the correction due to the second term on the right hand side of Eq. (13) can be neglected, and R_h should obey $R_h \sim N^{\nu}$. However, in this work, the chain length is not always large enough. Thus the scaling of R_h cannot be obtained in the whole range of N.

For $R_g^{-1} \ll k \ll a^{-1}$ (a being a microscopic length scale of the order of a bond length), the static structure factor[4] should follow $S(k)/N \sim (kRg)^{-1/\nu}$. The relationship between $S(k)/N$ and kRg is shown in Fig. 3 for each chain topology, in which different symbols, representing the polymer chains with different N, almost fall on the same asymptotic curve. The Flory exponent ν therefore can be deduced from the curve, showing $\nu=0.595$ for the ring-shaped polymer chain, $\nu=0.582$ for the three-arm branched chain, and $\nu=0.585$ for the linear chain in solution. The values of ν obtained from the static structure factor are systematically smaller than

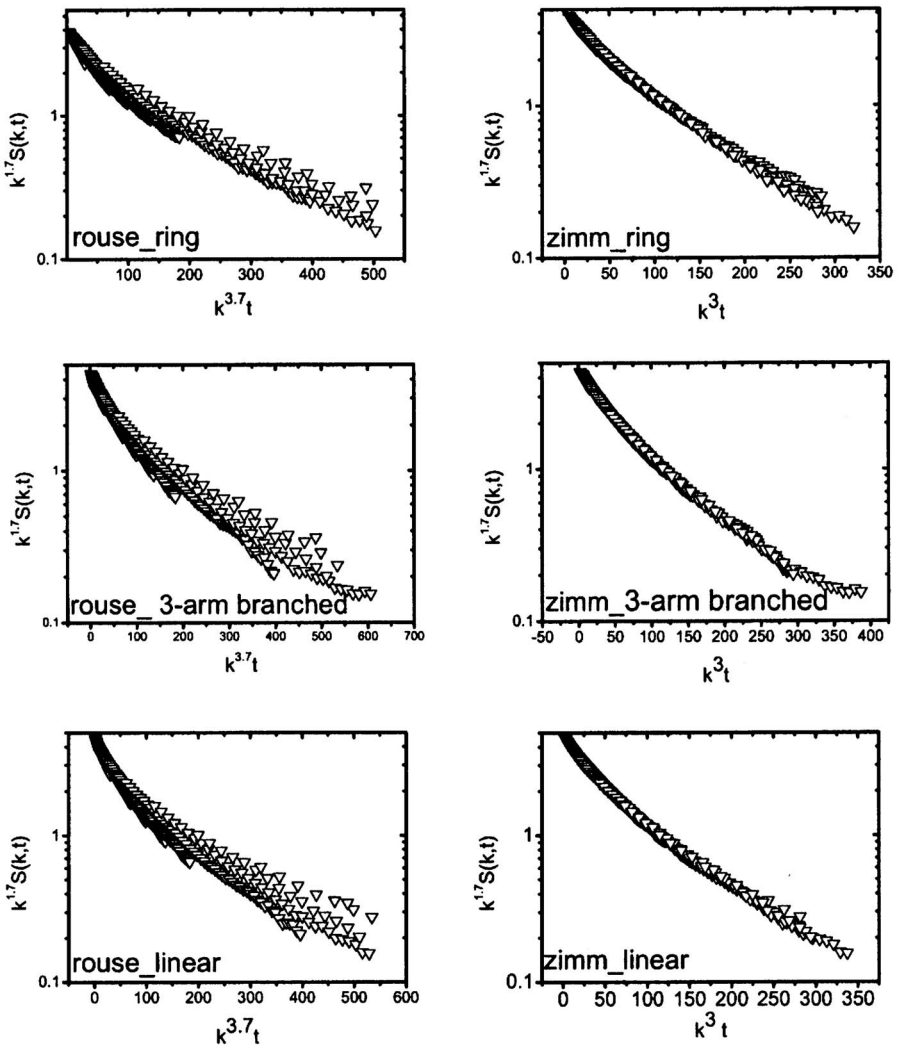

FIG. 7. The dynamic structure factor weighted by $k^{1.7}$ as a function of time t weighted by k^z for the ring-shaped, the three-arm branched, and the linear chains with $N=80$.

those from the R_g measurements. Specifically, ν value obtained from the static structure factor is 5% smaller than that from R_g measurements for the linear chain, whereas the difference between the scaling exponent from the static structure factor and that from R_g is negligible for the ring-shapedpolymer chain. This is possibly because the ring-shaped chain is more compact due to constraint; thus its conformation does not change drastically during simulations.

B. The dynamic properties

The diffusion coefficient and the relaxation time of the ring-shaped, the three-arm branched, and the linear polymer chains in solution are calculated. Their values are listed in Table I and shown in Fig. 4. Apparently, the ring-shaped chain diffuses faster than the three-arm branched and the linear chains. With increasing N, the diffusion coefficients of the three types of polymer chains decrease rapidly, and the difference between their values also reduces. It implies that, as long as the polymer chain is long enough (but still in the dilute solution regime), the influence of the topology on the diffusion of the polymer chain will vanish. Figure 4(b) shows that the relaxation time increases drastically with increasing N. This is because the larger the degree of polymerization is, the greater the discrepancies of R_g among different types of polymer chains are (see Fig. 1), while the values of the diffusion coefficient are similar.

Figures 5 and 6 show the scaling $D_{\text{c.m.}} \sim N^{-0.749}$ and $\tau \sim N^{1.947}$ for the ring-shaped chain, $D_{\text{c.m.}} \sim N^{-0.743}$ and $\tau \sim N^{1.933}$ for the three-arm branched chain, and $D_{\text{c.m.}} \sim N^{-0.758}$ and $\tau \sim N^{1.986}$ for the linear chain in solution. When the topology of the polymer chain is changed from linear to ring-structured or three-arm branched shape, the dynamic scaling exponent ν_d for diffusion coefficient $D_{\text{c.m.}}$ increases slightly, and the scaling exponent for τ decreases slightly. This can also be attributed that, as compared to the linear chain, the ring-shaped chain possesses no free ends and the three-arm branched chain has grafting point which limits the movement of chains.

The polymer dynamics in dilute solution is well described by the Zimm model,[18] in which the diffusion coefficient is

$$D_Z = \frac{k_B T}{\eta_s R_g} \sim N^{-\nu_d}, \tag{14}$$

where η_s is the viscosity of the solvent. Apparently, the dynamic scaling exponent ν_d is $\nu_d = -\nu$ in the Zimm model, in constrast to $\nu_d = -1$ in the Rouse model.[18]

For $R_g^{-1} \ll k \ll a^{-1}$ and the same period of time, the dynamic structure factor[11] obeys the following relation:

$$S(k,t) = k^{-1/\nu} f(k^z t)$$
$$\text{where } z = \begin{cases} 3.0 & \text{for the Zimm model} \\ 2 + 1/\nu & \text{for the Rouse model.} \end{cases} \quad (15)$$

We therefore plot $S(k,t)k^{1/\nu}$ as a function of $k^z t$ in Fig. 7 and find that all the data points almost fall onto a curve that best describes the Zimm model, while these data points cannot be described by the curve for the Rouse model. The dynamic scaling exponent and the dynamic structure factor all indicate the Zimm-like behavior of the three types of polymer chains in dilute solution.

IV. SUMMARY

The static and dynamic properties of the ring-shaped, the three-arm branched, and the linear polymer chains in solution are investigated using MD simulation method. At the same length, polymer chains with different topologies possesses different sizes and diffusion coefficients. Moreover, the static and dynamic scaling relationships of the polymer chain in solution are slightly influenced by the chain topology.

At the same N, the ring-shaped chain possesses the smallest size and largest diffusion coefficient. With increasing N, the difference of the radii of gyration between the three types of polymer chains increases, whereas the difference of the diffusion coefficients among them decreases. However, the influence of the molecular topology on the static and the dynamic scaling exponents is small. The static scaling exponents decrease slightly, and the dynamic scaling exponents increase slightly, when the topology of the polymer chain is changed from linear to ring-structured or three-arm branched shape. The dynamics of these three types of polymer chains in solution is Zimm-like according to the dynamic scaling exponents and the dynamic structure factors.

ACKNOWLEDGMENTS

This work is supported by the National Natural Science Foundation of China (20574070, 20674086, 20490220, and 20620120105) Programs and the Fund for Creative Research Groups (50621302), and subsidized by the Special Funds for National Basic Research Program of China (2005CB623800).

[1] S. Brown and G. Szamel, J. Chem. Phys. **109**, 6184 (1999).
[2] S. Brown and G. Szamel, J. Chem. Phys. **108**, 4705 (1998).
[3] K. Hur, R. G. Winkler, and D. Y. Yoon, Macromolecules **39**, 3975 (2006).
[4] M. Müller, J. P. Winttmer, and M. E. Cates, Phys. Rev. E **53**, 5063 (1996).
[5] S. Brown, T. Lenczycki, and G. Szamel, Phys. Rev. E **63**, 052801 (2001).
[6] J. M. Deutsch, Phys. Rev. E **59**, 2539 (1999).
[7] A. Bensafi, U. Maschke, and M. Benmouna, Polym. Int. **49**, 175 (2000).
[8] S. Brown and G. Szamel, Macromol. Theory Simul. **9**, 14 (2000).
[9] A. Sikorski, Makromol. Chem., Theory Simul. **2**, 309 (1993); A. Sikorski, *ibid.* **2**, 309 (1993).
[10] G. S. Grest, K. Kremer, S. T. Milner, and T. A. Witten, Macromolecules **22**, 1904 (1989).
[11] B. Dünweg, J. Chem. Phys. **99**, 6983 (1993).
[12] B. Dünweg and K. Kremer, Phys. Rev. Lett. **66**, 2996 (1991).
[13] B. H. Zimm and W. H. Stockmayer, J. Chem. Phys. **17**, 1301 (1949).
[14] M. P. Allen and D. J. Tildesley, *Computer Simulation of Liquids* (Clarendon, Oxford, 1987).
[15] H. J. C. Berendsen, J. P. M. Postma, W. F. van Gunsteren, and J. R. H. A. DiNola, J. Chem. Phys. **81**, 3684 (1984).
[16] O. Punkkinen, E. Falck, I. Vattulainen, and T. Ala-Nissila, J. Chem. Phys. **122**, 094904 (2005).
[17] M. Doi and S. F. Edwards, *The Theory of Polymer Dynamics* (Clarendon, Oxford, 1986).
[18] M. Rubinstein and R. H. Colby, *Polymer Physics* (Oxford University, Oxford, 2003).
[19] J. J. Prentis, J. Chem. Phys. **76**, 1574 (1981).
[20] C. J. C. Edwards, D. Rigby, and R. F. T. Stepto, Polymer **24**, 395 (1983).
[21] B. Dünweg, D. Reith, M. Steinhauser, and K. Kremer, J. Chem. Phys. **117**, 914 (2002).